

Spectral modeling of gaseous metal disks around DAZ white dwarfs

Klaus Werner, Thorsten Nagel, and Thomas Rauch

Institute for Astronomy and Astrophysics, Kepler Center for Astro and Particle Physics,
University of Tübingen, Germany

E-mail: werner@astro.uni-tuebingen.de

Abstract. We report on our attempt for the first non-LTE modeling of gaseous metal disks around single DAZ white dwarfs recently discovered by Gänsicke et al. and thought to originate from a disrupted asteroid. We assume a Keplerian rotating viscous disk ring composed of calcium and hydrogen and compute the detailed vertical structure and emergent spectrum. We find that the observed infrared Ca II emission triplet can be modeled with a hydrogen-deficient gas ring located at $R = 1.2 R_{\odot}$, inside of the tidal disruption radius, with $T_{\text{eff}} \approx 6000$ K and a low surface mass density of $\approx 0.3 \text{ g/cm}^2$. A disk having this density and reaching from the central white dwarf out to $R = 1.2 R_{\odot}$ would have a total mass of $7 \cdot 10^{21}$ g, corresponding to an asteroid with ≈ 160 km diameter.

1. Introduction: Dust around DAZ white dwarfs

More than two decades ago Zuckerman & Becklin (1987) announced the discovery of an IR excess around the DAZ white dwarf G29–38. The white dwarf itself is enriched in metals. Considering the short sedimentation timescales in the photosphere this implies that the star is accreting matter at a relatively high rate (Koester et al. 1997). Since no cool companion has been found at G29–38, the hypothesis was put forward that a dust cloud around the white dwarf causes the IR excess. In fact, the presence of dust has been confirmed by *Spitzer* observations (Reach et al. 2005). Graham et al. (1990) concluded that the dust is located in the equatorial plane. Subsequently, further DAZ white dwarfs with potential dust disks were found (Becklin et al. 2005, Kilic et al. 2005, 2006). As a possible origin of these disks tidally disrupted comets were discussed (Debes & Sigurdsson 2002) and, more likely because of the absence of H and He, disrupted asteroids (Jura 2003).

2. Gas disks around DAZ white dwarfs

Recently, signatures of a gas disk were discovered in Sloan Digital Sky Survey (SDSS) spectra of two DAZ white dwarfs (Gänsicke et al. 2006, 2007). The spectra display double-peaked emission lines of the infrared Ca II triplet $\lambda\lambda$ 8498, 8542, 8662 Å.

In the present paper, we concentrate on one of these two white dwarfs, namely SDSS 1228+1040, because its emission line profiles are more prominent. The white dwarf's atmospheric parameters are $T_{\text{eff}} = 22\,020$ K and $\log g = 8.24$. The derived stellar mass $M_{\text{WD}} = 0.77 M_{\odot}$ and radius $R_{\text{WD}} = 0.011 R_{\odot}$ are quantities that enter our disk model. The photospheric magnesium abundance is 0.8 times solar. The spectrum neither exhibits radial

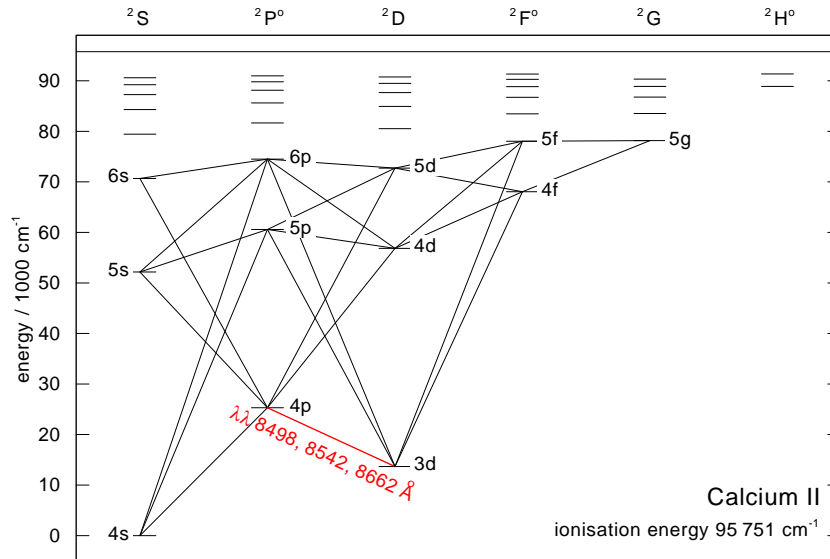


Figure 1. Grotrian diagram of our Ca II model ion. All highly excited levels that are not linked by radiative line transitions are treated in LTE. The 3d–4p transition causes the observed IR triplet.

velocity variations nor photometric variability. Besides the calcium emission lines only two other weaker emission features are seen (Fe II $\lambda\lambda$ 5018, 5169 Å). In particular, hydrogen and helium emissions are not discovered. It is concluded that the Ca and Fe emission lines stem from a metal-rich Keplerian disk around a single white dwarf. The Ca II line profiles are double peaked emission lines with a peak-to-peak separation of 630 km/s, i.e., the Keplerian rotation velocity is $v \sin i = 315$ km/s. There is a clear violet/red asymmetry in the double-peaked profiles, well known from a similar phenomenon in Be star disks that is ascribed to one-armed spiral waves.

From a spectral analysis with a kinematical LTE emission model Gänsicke et al. (2006) conclude that we see a geometrically thin, optically thick disk at high inclination ($i = 70^\circ$). The inner and outer disk radii are $R_{\text{in}} = 0.64 R_\odot$ and $R_{\text{out}} = 1.2 R_\odot$, respectively. While the outer disk radius is quite sharply confined because of the steep line wings, the value derived for the inner disk radius possibly just marks the inner edge of the Ca II line emission region and not the physical inner disk edge, i.e., R_{in} could reach down to the white dwarf’s surface. They also conclude that the gas temperature in the disk is around 4500–5500 K. Since the tidal disruption radius for a rocky asteroid at the white dwarf is $R \approx 1.5 R_\odot$, it is possible that the material in the gas disk may be a disrupted asteroid whose dust was sublimated by the white dwarf’s radiation field. It seems that SDSS 1228+1040 could be the hot counterpart to G29–38 and other cool DAZ stars harboring dust disks, but in the meantime DAZ white dwarfs with a dust disk and as hot as SDSS 1228+1040 were discovered (e.g., Jura et al. 2007).

It is our aim to compute a more realistic model for the gas disk around SDSS 1228+1040 and we are reporting here very first provisional results.

3. A viscous disk ring model

Basically we assume a Shakura & Sunyaev (1973) α -disk model, i.e., a geometrically thin Keplerian disk heated by viscosity. For numerical calculations we employ AcDc, our *Accretion Disk code* that we developed for modeling disks in cataclysmic variables and low-mass X-ray binaries (Nagel et al. 2004). The code computes a detailed vertical structure and the spectrum of

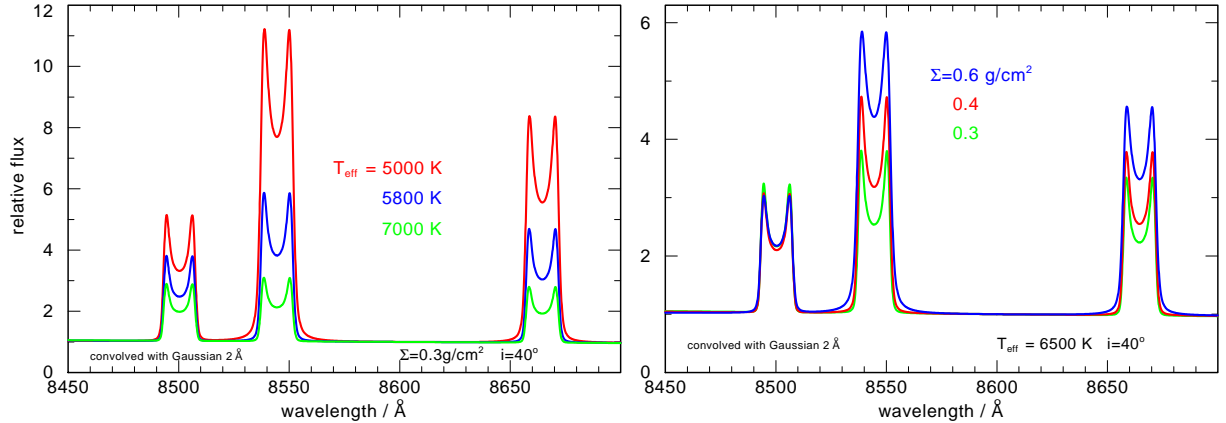


Figure 2. *Left:* T_{eff} dependence of the Ca II triplet emitted by a Keplerian rotating gas ring seen at an inclination angle $i = 40^\circ$. The emission becomes weaker with increasing T_{eff} . At the same time, the relative strengths of triplet components become equal. *Right:* A similar effect is seen when the surface mass density Σ decreases. Values for the ring parameters T_{eff} and Σ are given in the panels. All profiles are convolved with a 2 \AA FWHM Gaussian.

a disk which is being built from radial-symmetric annuli. For any disk annulus we assume that it radiates like a plane-parallel slab in non-LTE, and in radiative and hydrostatic equilibrium. We are presenting here the results of a single disk ring using different values for the input parameters T_{eff} (as a measure for the viscously dissipated energy) and surface mass density Σ (the vertical mass column from the disk midplane to the surface). Further input parameters, which are kept fixed, are white dwarf's mass and radius as given above, and $R_{\text{in}} = 91 R_{\text{WD}}$ and $R_{\text{out}} = 109 R_{\text{WD}}$ for the inner and outer disk radii, respectively. The chemical composition is calcium dominated with an admixture of hydrogen with varying H/Ca abundance ratios in order to determine the extent of H-deficiency.

The principal problem for any modeling attempt is posed by the question: what heats the Ca II emission line region? Although being hot, it cannot be the white dwarf because it is too distant. Also, it cannot be gravitational energy released through viscosity because the required mass-accretion rate would be $\approx 10^{-8} M_{\odot}/\text{yr}$ which is by many orders of magnitude larger than the accretion rate invoked for the presence of settling metals in DAZ photospheres ($\approx 10^{-15} M_{\odot}/\text{yr}$, Koester & Wilken 2006). A speculation by Jura (2008) is additional heating by energy dissipation through disk asymmetries, being driven by some external unseen planet. As mentioned above, such an asymmetry is obvious from the line profiles. Whatever, at the moment we do not know the heating mechanism. Therefore we need to use T_{eff} as a free parameter for the disk ring. *In praxi* this means that we set the accretion rate \dot{M} , which is related to T_{eff} through

$$T_{\text{eff}}^4(R) = [1 - (R_{\text{WD}}/R)^{1/2}] 3GM_{\text{WD}}\dot{M}/8\pi R^3,$$

to an artificially high value.

The calcium model atom used for the non-LTE calculations comprises three ionisation stages, Ca I–III with 7, 12, 1 non-LTE levels and 3, 26, 0 radiative line transitions, respectively. For the disk model calculations we do not account for level fine structure splitting. For the Ca II IR triplet this is done in the final formal solution of the transfer equation by distributing the level populations over the fine structure levels according to their statistical weight. Fig. 1 is a Grotrian diagram of our Ca II model ion with all implemented levels and lines, indicating the transition responsible for the observed IR triplet.

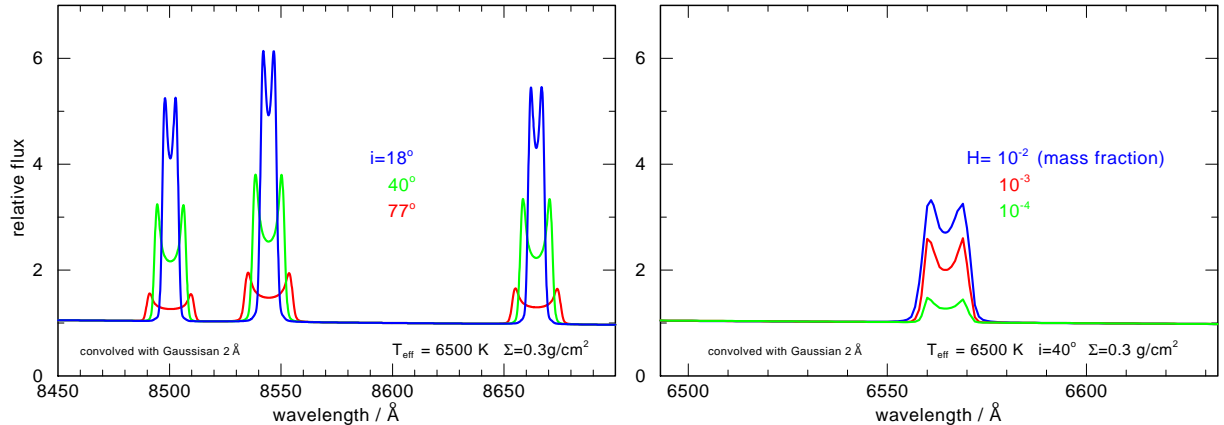


Figure 3. *Left:* The Ca II line shape of a particular model ($T_{\text{eff}} = 6500 \text{ K}$, $\Sigma = 0.3 \text{ g/cm}^2$) seen under different inclination angles i . The relative strength of the profile depression between double peaks increases with i . *Right:* H α line shape of the same model but with different hydrogen content. $H > 1\%$ would be detectable in SDSS 1228+1040.

Energy levels were taken from NIST, and oscillator strengths and photoionisation cross-sections from the Opacity and Iron Projects. Electron collisional rates are computed from usual approximation formulae. Rates for collisions with H are currently neglected, probably without consequences. That is because, first, Mashonkina et al. (2007) have shown that these collisions are unimportant in F/G type stars (having similar physical conditions in their photospheres) and, second, we are faced here with a H-deficient environment. Collisions of Ca with heavy ions are neglected, too. Their rates are unknown but probably unimportant because of the low thermal velocities of the perturbers. For the spectral lines we assume Voigt profiles with radiation damping parameters. Future improvement should include Van der Waals damping, although we don't expect it to be important in the disk environment. The hydrogen model atom is a standard configuration with ten non-LTE levels that we use routinely for stellar spectral modeling.

4. Results

We present first results from disk ring models for SDSS 1228+1040, discussing:

- the influence of T_{eff} , Σ , and inclination i on emergent line profiles of the Ca II IR triplet;
- an upper limit for hydrogen content from H α ;
- the characteristics of one representative model, in particular its vertical structure;
- a comparison of the computed spectrum with observation.

4.1. Influence of T_{eff} , Σ , i on the infrared Ca II triplet

In Fig. 2 (left panel) we see that the emission strength of the Ca II triplet decreases with increasing T_{eff} (with $\Sigma = 0.3 \text{ g/cm}^2$ kept fixed). This is because of the shifting Ca II/Ca III ionisation balance. A closer comparison of the three triplet components shows that the relative strengths of the components become equal with increasing T_{eff} , a behaviour that constrains T_{eff} from the observed line strengths. A similar trend is seen (Fig. 2, right panel) when Σ is reduced (with $T_{\text{eff}} = 6500 \text{ K}$ kept fixed). We stress that the models have a considerable continuum flux compared to line emission peak heights.

In Fig. 3 (left panel) we demonstrate that in principle the inclination angle can be constrained from the Ca II triplet line shape. Obviously, the relative strength of the profile depression between

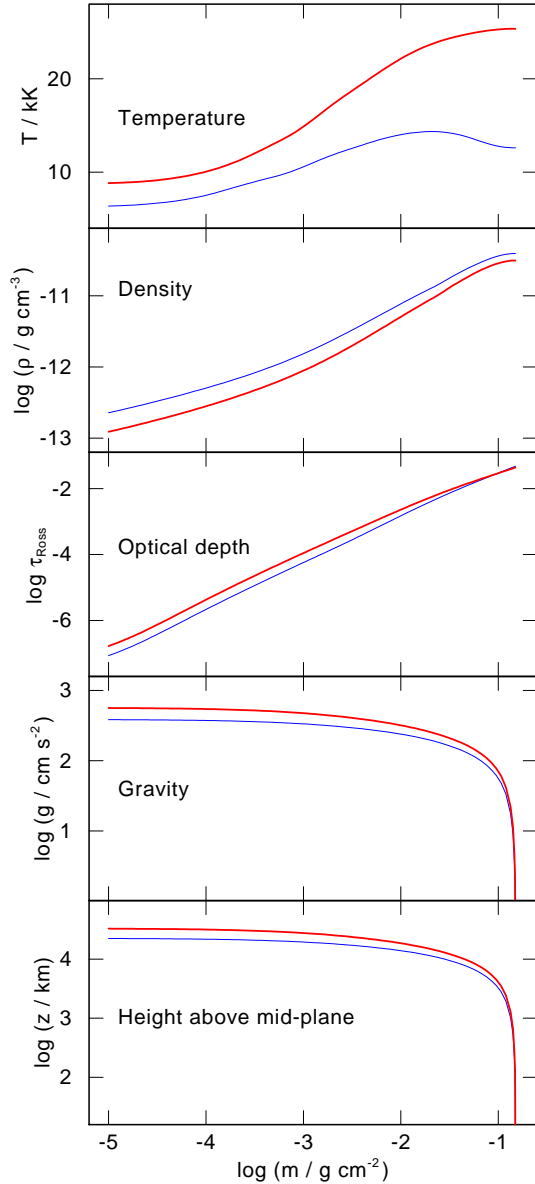


Figure 4. (Left) Vertical structure of two models ($T_{\text{eff}} = 5000$ K, thick lines, and 7000 K) with $\Sigma = 0.3$ g/cm². The run of various physical quantities is shown on a column-mass scale measured from the disk surface (left) to the disk midplane (right); see discussion in the text (Sect. 4.3). The disks are optically thin ($\tau_{\text{Ross}} < 0.1$).

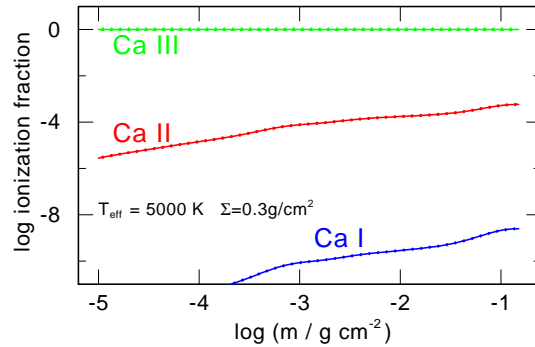


Figure 5. (Above) Vertical run of the calcium ionisation fractions in the model with $T_{\text{eff}} = 5000$ K and $\Sigma = 0.3$ g/cm². Ca III is the dominant ionisation stage.

the double peaks increases with inclination.

4.2. Upper limit for hydrogen

From the lack of H α emission in the spectrum of SDSS 1228+1040 we can make a quantitative estimate of the hydrogen-deficiency in the gas disk. Fig. 3 (right panel) depicts the H α line shape of a particular model in which we varied the H content (H = 1%, 0.1%, 0.01%; mass fraction). With an abundance of 1% the H α peak height is comparable to that of the Ca II triplet and, hence, would be detectable in the spectrum of SDSS 1228+1040.

4.3. Vertical structure of disk ring

Let us inspect the vertical structure of two representative ring models with different effective temperature displayed in Fig. 4. The range of temperature T and mass density ρ is comparable to the circumstances encountered in the atmospheres of F/G-type giants. Accordingly, the gravity increases from the disk midplane toward the disk surface, up to $\log g \approx 2.5$. The run

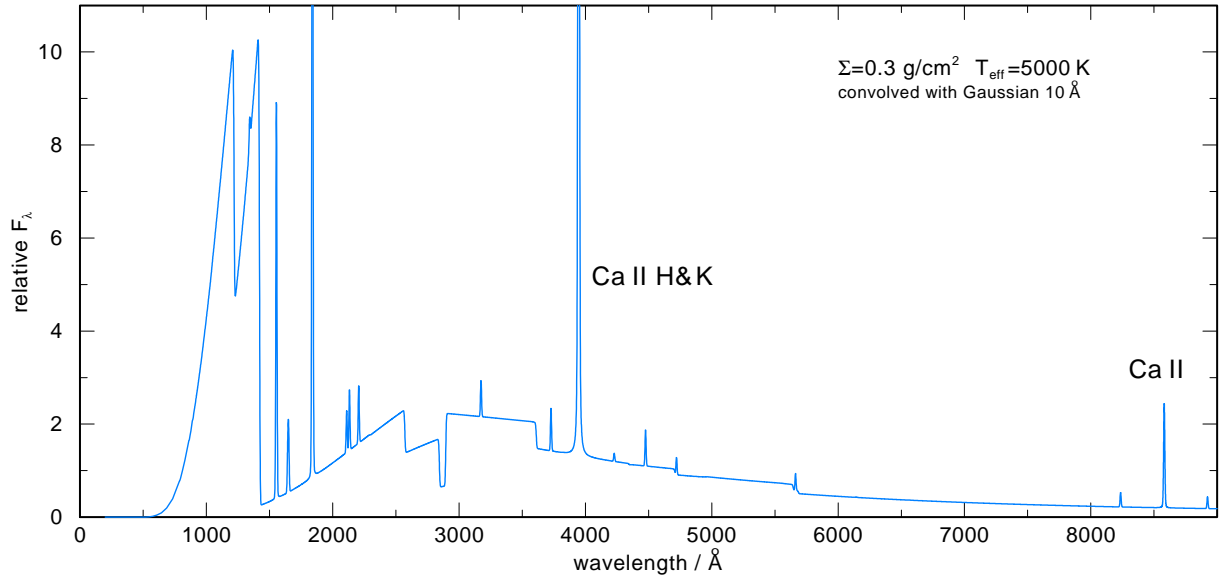


Figure 6. Flux distribution in the UV/optical range of the $T_{\text{eff}} = 5000 \text{ K}$, $\Sigma = 0.3 \text{ g/cm}^2$ model (no fine structure splitting applied to lines). The spectrum is dominated by Ca II emission lines and bound-free emission edges. The strongest feature is the H&K line. For the sake of clarity, the spectrum is convolved with a 10 \AA FWHM Gaussian.

of the Rosseland optical depth τ_{Ross} shows that the disks are optically thin. The geometrical height z above the midplane shows that the thickness of the disk ring is about $\Delta R = 50\,000 \text{ km}$, hence, $\Delta R/R \approx 15$. The non-LTE departure coefficients (not plotted) of the atomic population numbers in these two models deviate significantly from the LTE value $b = 1$. For the lower levels of the Ca II IR triplet in the $T_{\text{eff}} = 5000 \text{ K}$ model, for example, they range between $b \approx 0.001$ in the upper layers of the disk and $b \approx 50$ in deeper regions.

Fig. 5 shows the vertical calcium ionisation stratification for the cooler ($T_{\text{eff}} = 5000 \text{ K}$) of these two models. Ca III is by far the dominant ionisation stage everywhere in the model. This advises us to extend the model atom to include the next higher ionisation stage in future calculations, although we do not expect a dramatic depopulation of Ca III (and Ca II) because its ionisation potential is rather high (50.9 eV).

It is interesting to look at the overall flux spectrum of the models, e.g., Fig. 6. The spectrum is dominated by Ca II emission lines. The Ca II H&K resonance doublet is by far the strongest emission feature that should be detectable in the spectrum of SDSS 1228+1040, although the WD flux increases by about an order of magnitude from the location of the IR triplet to the H&K line. A close inspection of the residual disk spectrum of SDSS 1228+1040 (i.e., observation minus WD model spectrum) presented by Gänsicke et al. (2008) indeed displays an emission feature at the location of the H&K line, although not explicitly described by the authors. In a new high-quality spectrum of SDSS 1228+1040 (Gänsicke, this meeting) the presence of this emission line is clearly confirmed. It seems, however, that the observed strength is strongly overestimated by our models, a result that also holds for the LTE emission models presented by Gänsicke.

Another remarkable feature of the overall model flux spectrum in Fig. 6 is the occurrence of two prominent Ca II *emission edges* at 1219 \AA and 1420 \AA , created by recombination processes into the first and second excited states, respectively. These features should be easily detectable in UV spectra as well as many other emission lines from other metals as predicted and presented

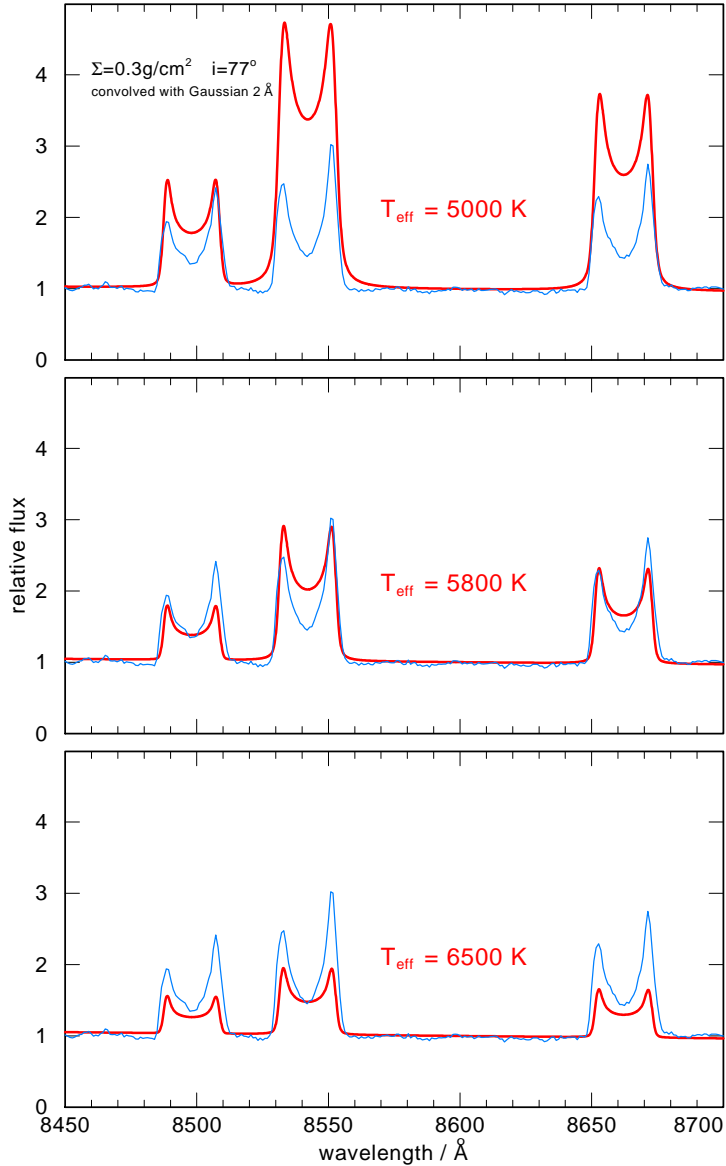


Figure 7. Normalized spectra of three models (thick lines) with different T_{eff} compared to the observed spectrum of SDSS 1228+1040. The fitting procedure is ambiguous because the observation is normalized to the continuum that is probably dominated by the white dwarf. All models have $\Sigma = 0.3 \text{ g/cm}^2$ and are viewed at an inclination of $i = 77^\circ$.

by Gänsicke at this meeting. Our models promise that the proposed (and approved) HST/COS spectroscopic observation of SDSS 1228+1040 by Gänsicke and collaborators will deliver an exciting dataset that will allow important conclusions on the chemical composition of the gas disk.

4.4. Models vs. observation

In Fig. 7 we show a direct comparison of the normalised spectrum of SDSS 1228+1040 to three models with different effective temperatures. This comparison is, however, complicated by the fact that Gänsicke et al. (2006) suggest that the continuous radiation in the vicinity of

the Ca II triplet stems from the white dwarf alone, while in contrast our models predict a non-negligible contribution by the disk. What we compare in Fig. 7 is the observed spectrum normalized to the WD (+disk) continuum and the computed disk spectrum alone, normalized to its emission continuum. In any case, it can be seen that the effective temperature of the disk at SDSS 1228+1040 is well constrained by the three models, being $T_{\text{eff}} \approx 5800$ K. The cooler model ($T_{\text{eff}} = 5000$ K) is perhaps more favorable because of the larger line-to-continuum emission ratio, while the hotter model ($T_{\text{eff}} = 6500$ K) has the advantage that the relative strengths of the three line components are matched better.

5. Summary and conclusions

The infrared Ca II emission triplet in the spectrum of the DAZ white dwarf SDSS 1228+1040 can be modeled with a geometrically and optically thin, Keplerian viscous gas disk ring at a distance of $1.2 R_{\odot}$ from the WD, with $T_{\text{eff}} \approx 6000$ K and a low surface mass density $\Sigma \approx 0.3 \text{ g/cm}^2$. One serious open problem is the unknown disk-heating mechanism. The disk is hydrogen-deficient ($\text{H} \leq 1\%$ by mass) and it is located within the tidal disruption radius ($R_{\text{tidal}} = 1.5 R_{\odot}$). If one assumes that the disk reaches down to the WD and that it has uniformly this surface density, then its total mass would be $7 \cdot 10^{21}$ g. A rocky asteroid ($\bar{\rho} = 3 \text{ g/cm}^3$) with this mass would have a diameter of about 160 km. An asteroid of this size in our solar system is, e.g., 22 Kalliope.

Future work will include other abundant metal species, with a composition appropriate for asteroids. However, at the moment there are only two Fe II lines detected. Real progress for an abundance analysis of the gas disk around SDSS 1228+1040 is only possible with future UV spectroscopy.

While the determination of the composition of accreted material from abundance analyses in DAZ atmospheres is an indirect method that depends on our theoretical knowledge about metal settling timescales, the analysis of the gas disks has the obvious advantage that is a direct composition measurement.

Acknowledgments

We thank Boris Gänsicke for sending us his SDSS 1228+1040 spectrum in electronic form and for useful discussions. T.R. is supported by the *German Astrophysical Virtual Observatory* project of the Federal Ministry of Education and Research (grant 05 AC6VTB).

References

- Becklin, E. E., Farihi, J., Jura, M., Song, I., Weinberger, A. J., & Zuckerman, B. 2005, *ApJ*, 632, L119
 Debes, J. H., & Sigurdsson, S. 2002, *ApJ*, 572, 556
 Gänsicke, B. T., Marsh, T. M., Southworth, J., & Rebassa-Mansergas, A. 2006, *Science*, 314, 1908
 Gänsicke, B. T., Marsh, T. M., & Southworth, J. 2007, *MNRAS*, 380, L35
 Gänsicke, B. T., Marsh, T. M., Southworth, J., & Rebassa-Mansergas, A. 2008, preprint, arXiv:0710.2807v1
 Graham, J. R., Matthews, K., Neugebauer, G., & Soifer, B. T. 1990, *AJ*, 357, 216
 Jura, M. 2003, *ApJ*, 584, L91
 Jura, M., Farihi, J., & Zuckerman, B. 2007, *ApJ*, 663, 1285
 Jura, M. 2008, *AJ*, 135, 1785
 Kilic, M., von Hippel, T., Leggett, S. K., & Winget, D. E. 2005, *ApJ*, 632, L115
 Kilic, M., von Hippel, T., Leggett, S. K., & Winget, D. E. 2006, *ApJ*, 646, 474
 Koester, D., & Wilken, D. 2006, *A&A*, 453, 1051
 Koester, D., Provencal, J., & Shipman, H. L. 1997, *A&A*, 320, L57
 Mashonkina, L., Korn, A. J., & Przybilla, N. 2007, *A&A*, 461, 261
 Nagel, T., Dreizler, S., Rauch, T., & Werner, K. 2004, *A&A*, 428, 109
 Reach, W. T., Kuchner, M. J., von Hippel, T., et al. 2005, *ApJ*, 635, L161
 Shakura N. I., & Sunyaev, R. A. 1973, *A&A*, 24, 337
 Zuckerman, B., & Becklin, E. E. 1987, *Nature*, 330, 138